Supplement of Biogeosciences, 21, 843–868, 2024
https://doi.org/10.5194/bg-21-843-2024-supplement

Biogeosciences
Open Access

Supplement of

Enhanced net CO_2 exchange of a semideciduous forest in the southern Amazon due to diffuse radiation from biomass burning

Simone Rodrigues et al.

Correspondence to: George Vourlitis (georgev@csusm.edu)

S1 Supplementary Results

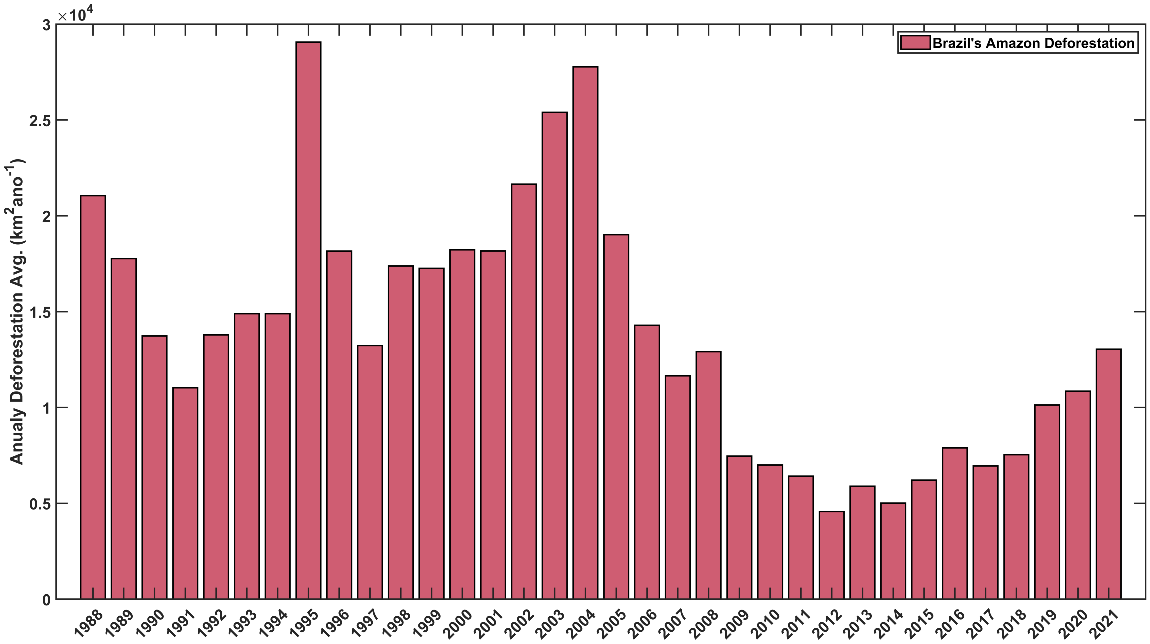

Fig. S1: Time series of clear-cut deforestation in the Legal Amazon (1988 to 2021). Data originated from the PRODES project. The data were collected at the website from The National Institute for Space Research (INPE), link in Table S5.

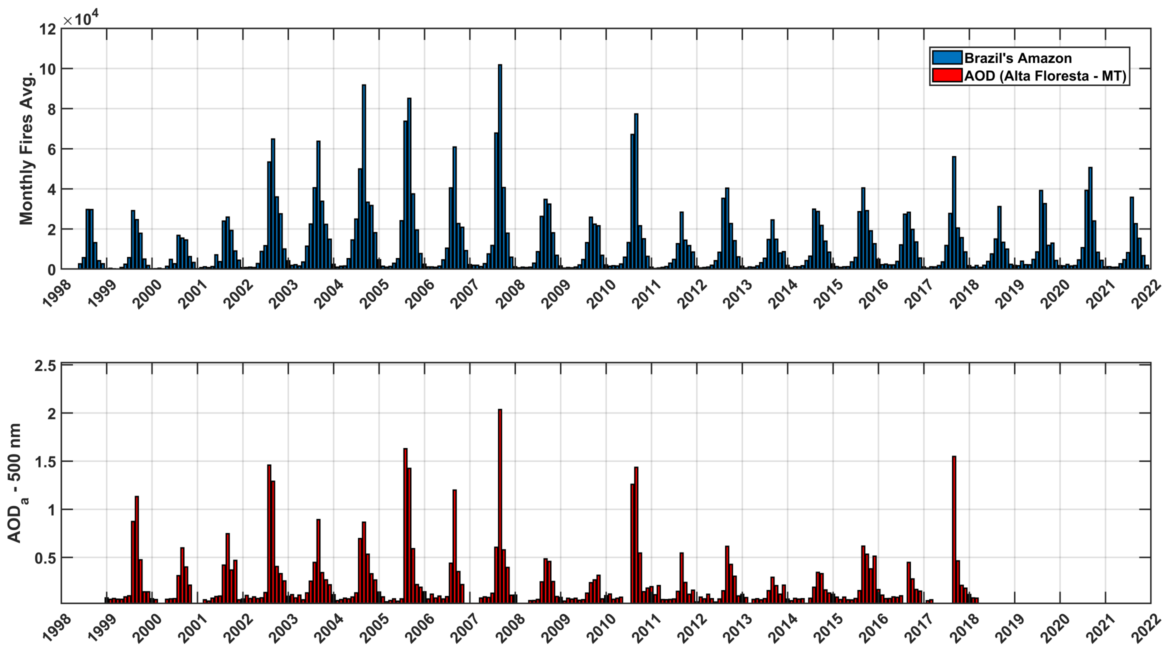

Fig. S2: Shows the time series of fires in the Legal Amazon from 1998 to 2022; data originated from the PRODES project (top panel). At the bottom panel, we show the time series of AOD (500 nm) for the Legal Amazon (1999 to 2017), originating from the AERONET solar photometer (on the ground), remote measurements managed by NASA. All data can be found in the links disposed in the Table S5.

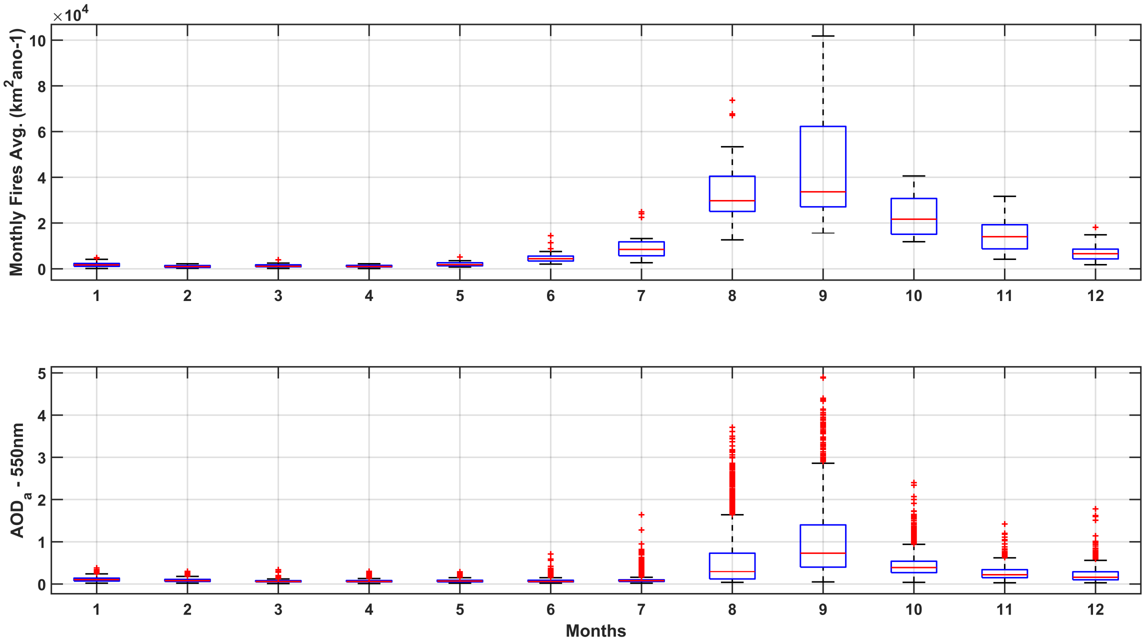

Fig. S3: In the image above, the boxplot shows the statistical behavior of the time series of monthly data on fires that occurred in the Legal Amazon (1998 to 2022). We observed an expressive seasonality from August to November, with a high peak occurrence during September. In the image below, the AOD at 550 nm (AQUA /TERRA) boxplot tracks the fire behavior for the same period. Additional results for fire numbers in the wet season and transitions are presented in Fig. S5.

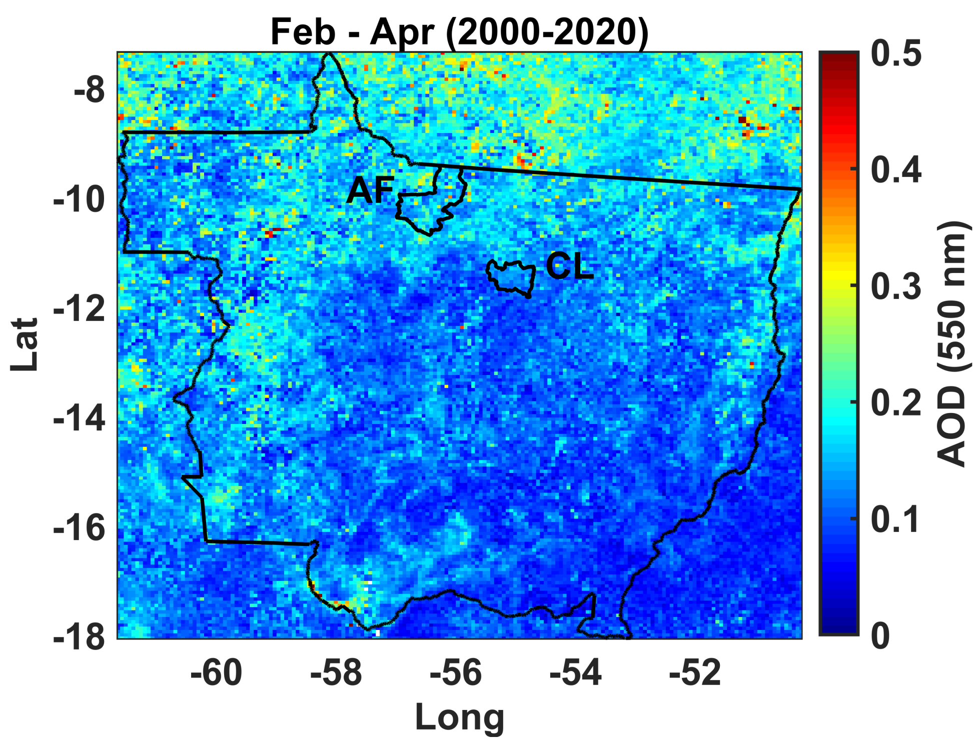

Fig. S4: Spatial behavior of aerosol optical depth (AOD) over the State of Mato Grosso (intense area of the arc of deforestation). In the image above is the behavior of AOD during the wet season (February to April) for the data period from 2000 to 2020, obtained from the AQUA and TERRA satellites.

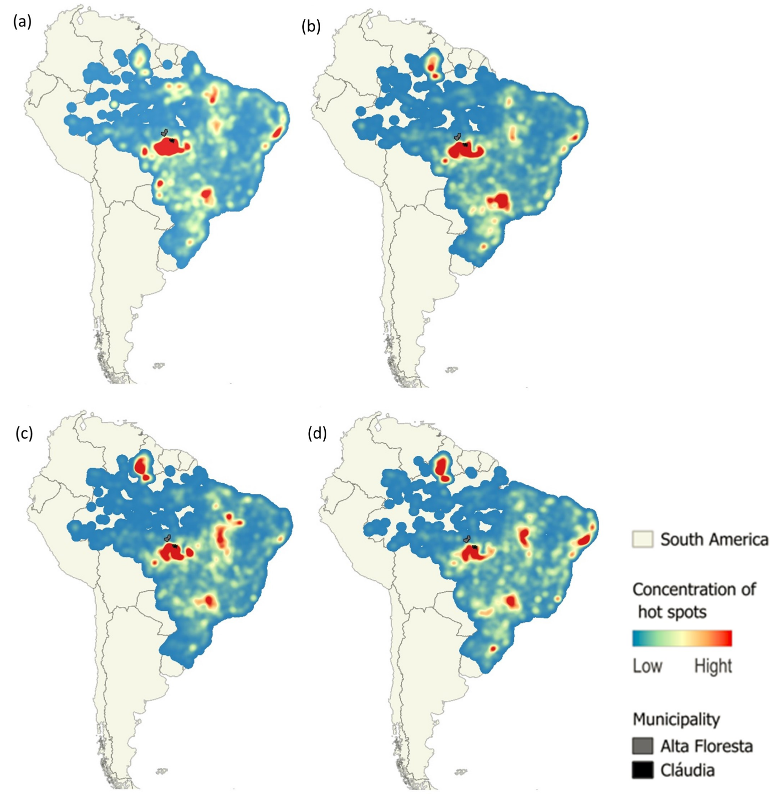

Fig. S5: Accumulated fire focus in Brazil for non-dry months. (a) Jan-Jun/2005, (b) Jan-Jun/2006, (c) Jan-Jun/2007 and (d) Jan-Jun/2008. Reference Satellite: MODIS/Aqua+Terra Thermal Anomalies/Fire locations 1 km FIRMS V0061 NRT (Vector data). Table S4 details the computed fire numbers to the wet season and transitions.

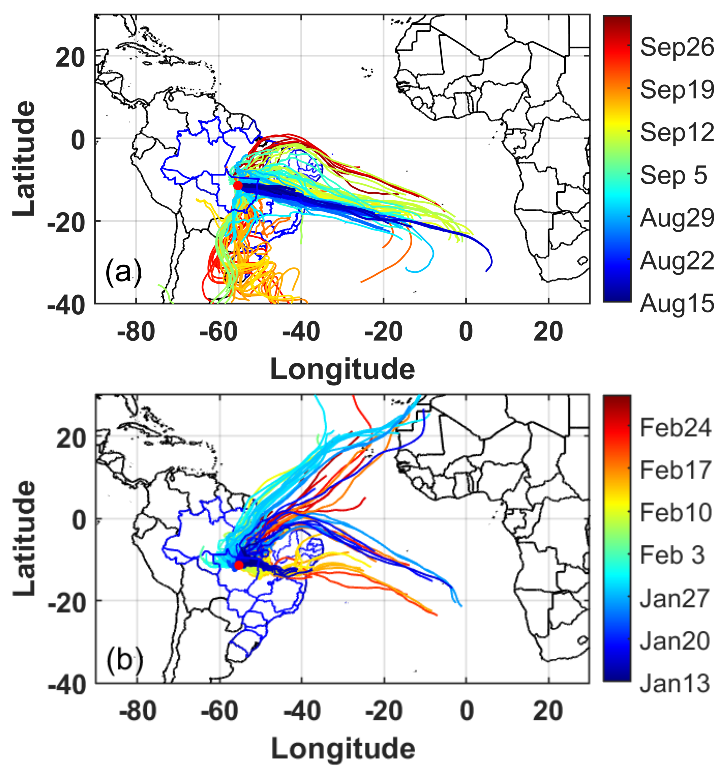

Fig. S6: Simulation of 14-day air mass backtrajectories using the HYSPLIT system during (a) Aug-Sep/2008 and (b) Jan-Feb/2008 (Claudia, Mato Grosso). Vertical air dispersion limited to 100 m.

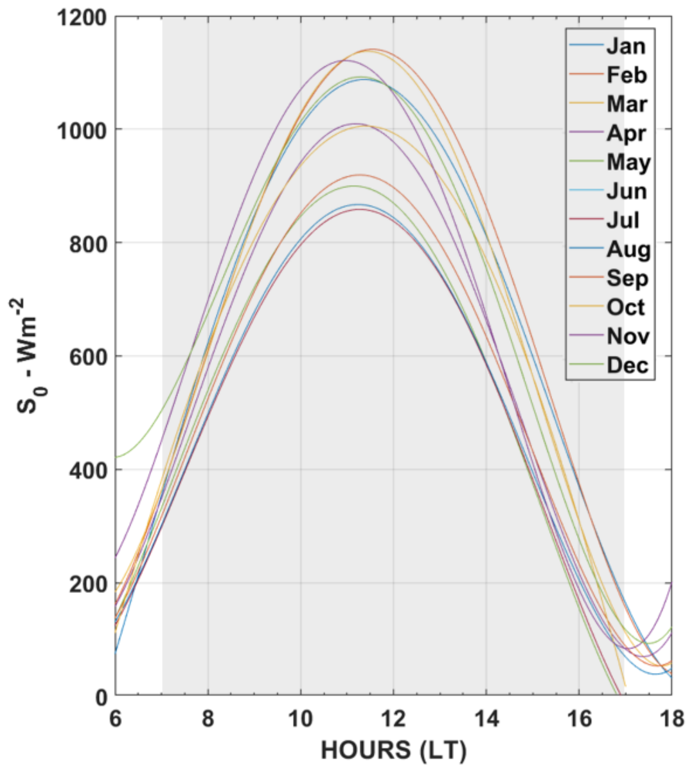

Fig. S7: Curves containing the average hourly behavior (monthly) of incident solar radiation values measured by AERONET in Alta Floresta-MT. The analyzed hourly values are between 07h and 17h (LT) from July 2005 to June 2008. We excluded from the data set all the values before 07h (LT) and after 17h (LT). Only the daylight hours are considered. Curve fits are listed in Table S1.

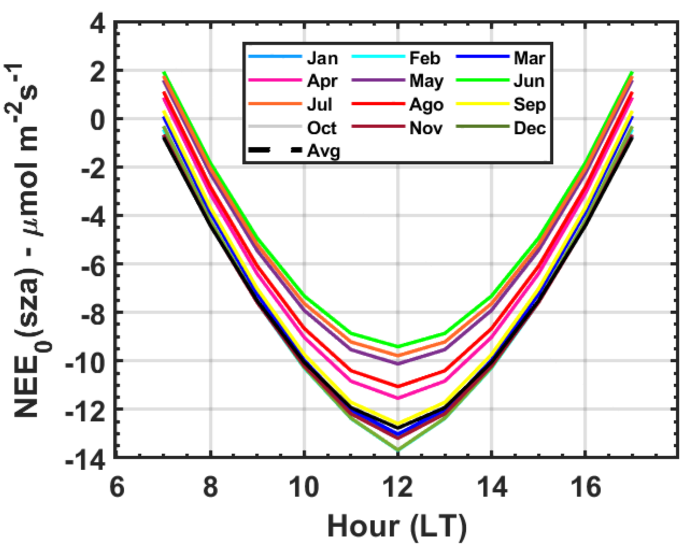

Fig. S8: Shows hourly cycle changes on the $NEE_0(sza)$. Fit curves under clear sky conditions (f ∼1.0) for each month of the year between Jul/2005-Jun/2008, 07-17h (LT). Curve fits are listed in Table S2.

S2 Additional Methods and Analyses

S2.1 Leaf Canopy Temperature -

Here, we call Leaf Canopy Temperature (LC_{Ts}) as a method using the Stefan-Boltzmann equation from the shortwave solar radiation measurements and longwave and albedo estimates as follows, Equation S1:

$$LC_{Ts} = \sqrt[4]{\left(\frac{SWi(1 - \alpha + LWa - Rn)}{\varepsilon\sigma}\right)} \tag{S1}$$

Where: Rn is the net radiation measured in the experimental area ($\mathrm{Wm^{-2}}$); α is the mean albedo of the leaf canopy during the dry and wet seasons, respectively equal to 0.079 and 0.126 [Marques et al., 2017]; LW_a is the atmospheric longwave radiation in $\mathrm{Wm^{-2}}$ [Idso and Jackson, 1969], adjusted for the polluted atmospheric conditions of Mato Grosso during the dry season [Von Randow, 2006]; ϵ is the emissivity, assumed to be 0.98 [Monteith and Unsworth, 1990, Marques et al., 2017] and, σ, the Stefan-Boltzmann constant (5.67×10^{-8} $\mathrm{Wm^{-2}\ K^{-4}}$). A similar method has been widely used, lacking direct leaf temperature measurements in the Amazon (Doughthy et al., 2010; Cirino et al., 2014; Andrade et al., 2021).

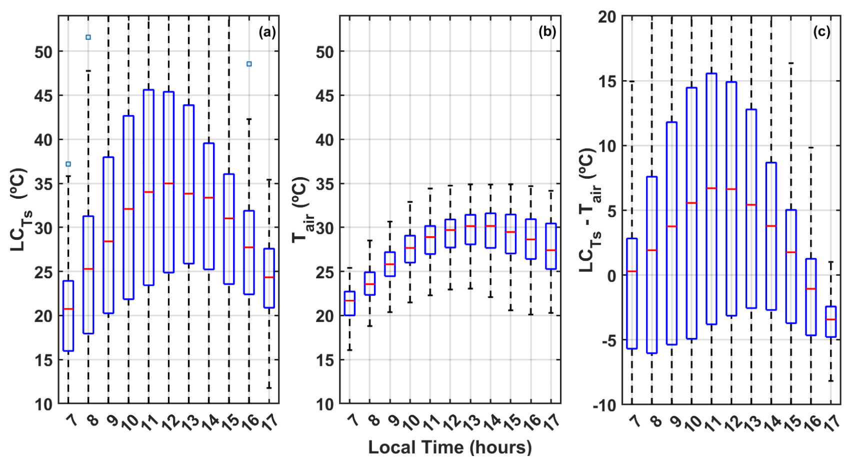

Fig. S9: Shows (a) the hourly cycle of leaf canopy temperature estimated from (Equation 1); (b) the hourly cycle of air temperature; and (c) the difference found between LC_{Ts} and T_{air} (°C), illustrating the warmest leaf canopy during daylight, between 07–17h (LT).

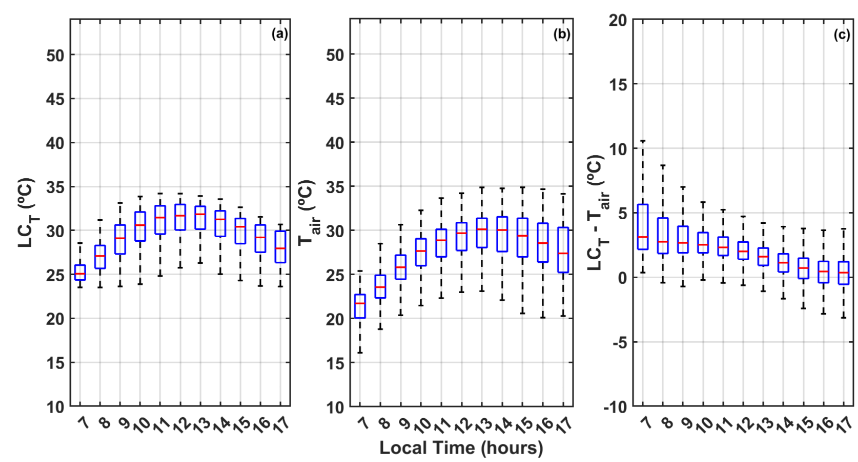

Fig. S10: (a) hourly cycle of leaf canopy temperature estimated by the LC_T model, Equation 9 (Tribusy, 2005); (b) the hourly cycle of air temperature; and (c) the difference found between LC_T and T_{air} (°C), indicating the warmest leaf canopy than the air between 07–17h (LT).

S2.2 Gross Primary Productivity (GPP) -

To compute GPP, we used the detailed procedures of [Wutzler et al., 2018] via the REddyProc package. The source code is available via the git revisioning system (Max Planck Institute - BGI). The code takes input from meteorological and flux variables such as SW_i, T_{air}, VPD, NEE, H, LE, and $u^{\star}$ from which are applied filtering methods $u^{\star} > 0.28$ [Papale et al., 2006, Barr et al., 2013] to correct underestimates at the nighttime R_{eco}. Moreover, the system estimates the threshold distribution for $u^{\star}$ to gap filling on the input data and then partitions the fluxes into NEE, GPP, and R_{eco}. The Look-up Tables – LUT, Mean Diurnal Course – MDC, and Marginal Distribution Sampling – MDS techniques are applied to the partitioning fluxes based on the meteorological conditions and carbon dioxide and water fluxes. REddyProc system takes advantage of these measurements to estimate the uncertainty of the hourly fluxes of our database. From Equation S2, we evaluated the GPP and, finally, the R_{eco}, calculated according to Equation S3. For the partitioning of fluxes, three methods are considered: the Look-Up Table (LUT), Mean Diurnal Course (MDC), and the Marginal Distribution Sampling (MDS) gap-filling method, which is currently the most commonly employed approach [Wutzler et al., 2018].

$$GPP = NEE - R_{eco} \tag{S2}$$

Where: GPP and R_{eco} are the Gross Primary Productivity and the ecosystem respiration (μmol m^{-2} s^{-1}), respectively (Wutzler et al., 2018).

$$R_{eco} = R_{ref} \cdot exp\left[E_0\left(\frac{1}{T_{ref} - T_0} - \frac{1}{T - T_0}\right)\right] \tag{S3}$$

Where: R_{eco} is given as a function of temperature sensitivity (E_0), T_0 is kept constant at $-$ 46.02 °C, and the reference temperature T_{ref} at 15 °C. The respiration at the reference temperature (R_{ref}) is recalculated based on nighttime data using the annual E_0 temperature sensitivity estimate [Reichstein et al., 2005]. This estimation is performed within 7-day windows that are sequentially shifted over a span of 4 days (Wutzler et al., 2018). Gap-filling hourly NEE data is imperative to obtain a complete time series for calculating daily averages or balances, such as monthly or seasonal sums. The REddyProc system implements the following three gap-filling methods.

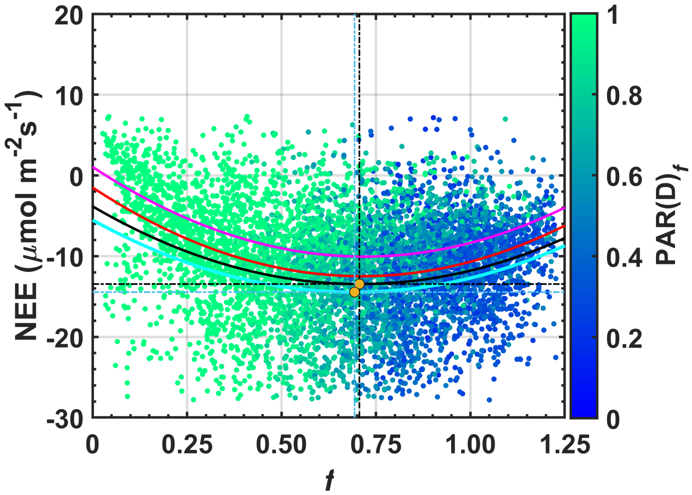

Fig. S11: Variability on the NEE for various SZA ranges (deg) during all the year (Jan-Dec/2005-2008), at Claudia, Mato Grosso: 0-20 (cyan), 20-40 (black), 40-60 (magenta), and 0-60 (red).

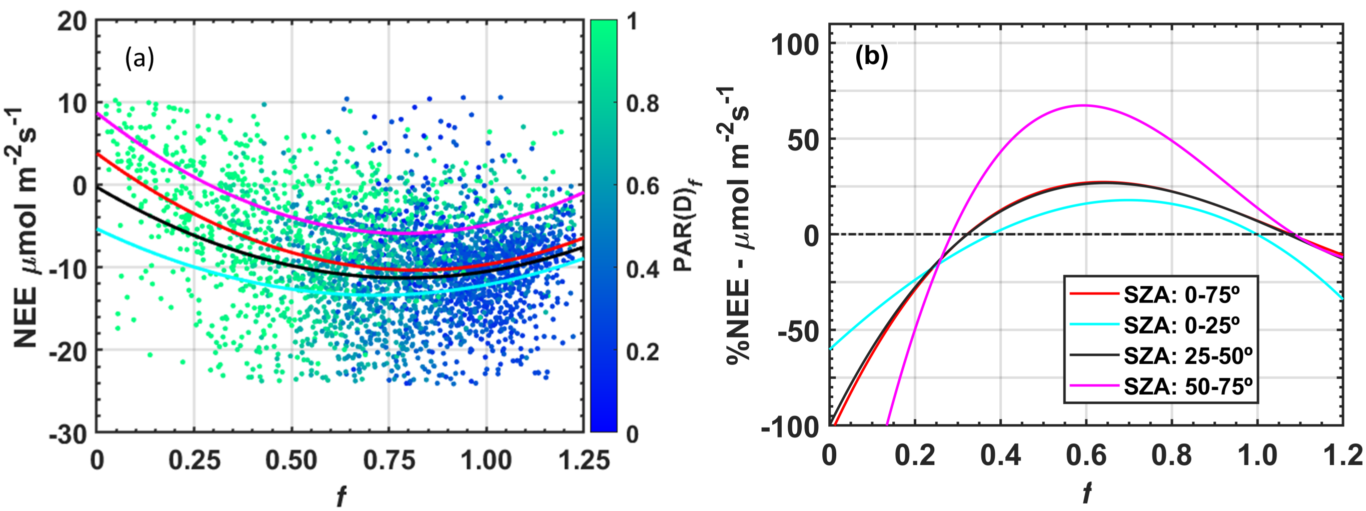

Fig. S12: (a) Variability on the NEE for various SZA ranges (deg) during the wildfire season (Jul-Nov/2005-2008), at Claudia, Mato Grosso: 0-20 (cyan), 20-40 (black), 40-60 (magenta), and 0-60 (red). Curve fits and tipping points (C_p) are listed in Table S3. (b) Shows relative change $\%NEE$ for the same period (Jul-Nov/2005-2008).

Table S1: Coefficients of the fitted curves of the average hourly (monthly) data of incident solar radiation values measured by AERONET in Alta Floresta-MT. The analyzed hourly values are between 07h and 17h (LT) for the period from July 2005 to June 2008.

4th degree polynomial curves					
Months	$p1$	$p2$	$p3$	$p4$	$p5$
January	$+0.38$	-17	$+2.4 \times 10^2$	-1.1×10^3	$+1.2 \times 10^3$
February	$+0.57$	-26	$+4.1 \times 10^2$	-2.4×10^3	$+4.7 \times 10^3$
March	$+0.69$	-32	$+4.9 \times 10^2$	-3.0×10^3	$+6.2 \times 10^3$
April	$+0.64$	-29	$+4.3 \times 10^2$	-2.5×10^3	$+5.0 \times 10^3$
May	$+0.44$	-20	$+2.9 \times 10^2$	-1.6×10^3	$+2.8 \times 10^3$
June	$+0.43$	-20	$+3.0 \times 10^2$	-1.7×10^3	$+3.1 \times 10^3$
July	$+0.49$	-22	$+3.3 \times 10^2$	-1.9×10^3	$+3.6 \times 10^3$
August	$+0.51$	-23	$+3.5 \times 10^2$	-2.0×10^3	$+3.8 \times 10^3$
September	$+0.15$	-07	$+8.8 \times 10^1$	-1.4×10^2	-8.7×10^2
October	$+0.77$	-34	$+5.1 \times 10^2$	-2.9×10^3	$+5.8 \times 10^3$
November	$+0.74$	-35	$+5.5 \times 10^2$	-3.5×10^3	$+8.1 \times 10^3$
December	-0.42	$+24$	-5.1×10^2	$+4.9 \times 10^3$	-1.6×10^4

Table S2: Coefficients of the $NEE_0(asz)$ curves adjusted monthly to clear sky conditions in the municipality of Claudia-MT between Jun/2005 and Jul/2008.

Months	p1	p2	p3	R^2	RMSE
January	$+0.0014$	$+0.0826$	-13.90	0.6	4.6
February	$+0.0054$	-0.3876	-04.60	0.4	5.6
March	$+0.0011$	$+0.1145$	-14.10	0.3	5.4
April	$+0.0033$	-0.0370	-13.50	0.5	5.8
May	$+0.0057$	-0.2150	-10.20	0.4	4.4
June	$+0.0091$	-0.6277	-01.00	0.2	7.2
July	$+0.0039$	-0.1793	-08.50	0.1	3.4
August	$+0.0058$	-0.2657	-08.60	0.4	5.3
September	$+0.0018$	$+0.0045$	-11.40	0.3	4.8
October	$+0.0015$	$+0.0762$	-14.10	0.4	5.4
November	$+0.0026$	$+0.0527$	-14.80	0.6	5.0
December	$+0.0117$	-0.7177	-03.40	0.8	4.0

Table S3: Polynomial adjustments, coefficients, and statistics between 07-17h (LT) in the micrometeorological tower 50 km from Sinop-MT, in the municipality of Cláudia-MT, between 2005-2008 (Figure S12a).

Settings	**Angles**		**Coeficientes**		**Statistic**
Poly fit 2nd	SZA	a	b	c	C_p (x_v,y_v)
	0-20°	+19	−26	−5.5	(0.68, −14.39)
NEE of CO_2	20-40°	+19	−27	−3.8	(0.71, −13.39)
	40-60°	+21	−31	+1.0	(0.73, −10.44)
	0-60°	+22	−31	−1.5	(0.70, −12.42)

Table S4: It lists the number of fire outbreaks recorded by the AQUA-TERRA space platforms during the years between 2005-2008 in the Amazon Basin. Where: 1 – flag to short no-dry-season; 2 – flag long no-dry-season. No-Dry means polluted-wet-season (BBOA), and Rel. Fire is ration or quotient (No-Dry/Dry-Season).

Yrs	**Fire Season**	**Dry Season**	**No-Dry$_1$**	**No-Dry$_2$**	**Rel. Fire$_1$**	**Rel. Fire$_2$**
-	**Jul-Dec**	**May-Sep**	**Jan-Apr & Dec**	**Jan-Apr & Oct-Dec**	**-**	**-**
2005	239,814	190,920	16,122	73,074	8%	38%
2006	155,304	117,881	12,710	58,227	11%	49%
2007	239,905	191,645	13,219	71,749	7%	37%
2008	120,156	73,640	10,399	60,853	14%	83%
Total	755,179	574,086	52,450	263,903	9%	46%

Table S5: List with hyperlinks (in blue) and Digital Object Identifiers (DOI) of all data used to figures and tables in this publication.

Open Research - Data Availability Statement				
Secondary Data	**Repository**	**Hyperlink**		**WebPage**
Remote Sensing (Satellites)	Terra-Aqua	Laads Daac	–	NASA Laads Daac
Remote Sensing (Ground)	Aeronet (Lev.2.0)	Goddard-Sfc	–	NASA Goddard
Short Wave Radiation	Aeronet (Lev.1.5)	Goddard-Sfc	–	NASA Goddard
Deforestation and fires	Prodes	Terra-Brasilis	–	INPE Prodes
Weather forecasts Models	Sol-Calculator	Solar-Calculator	–	METEO Exploration
Primary Data	**Repository**	**Hyperlink**	**DOI**	**Managers**
Eddy Flux (CO_2)	Mendeley Data	Brazil-EFlux-Stf	10.17632/m5h5fw872g.1	Cirino et al. (2022)
Net Ecosystem Exchange (NEE)	Mendeley Data	Brazil-NFlux-Stf	10.17632/m5h5fw872g.1	Cirino et al. (2022)
Meteorological Data	Mendeley Data	Brazil-AWsta-Stf	10.17632/m5h5fw872g.1	Cirino et al. (2022)

[Barr et al., 2013] Barr, A., Richardson, A., Hollinger, D., Papale, D., Arain, M., Black, T., Bohrer, G., Dragoni, D., Fischer, M., Gu, L., Law, B., Margolis, H., McCaughey, J., Munger, J., Oechel, W., and Schaeffer, K. (2013). Use of change-point detection for friction–velocity threshold evaluation in eddy-covariance studies. *Agricultural and Forest Meteorology*, 171-172:31–45.

[Idso and Jackson, 1969] Idso, S. B. and Jackson, R. D. (1969). Thermal radiation from the atmosphere. *Journal of Geophysical Research (1896-1977)*, 74(23):5397–5403.

[Marques et al., 2017] Marques, H. O., Biudes, M. S., Pavão, V. M., Machado, N. G., Querino, C. A. S., and Danelichen, V. H. d. M. (2017). Estimated net radiation in an Amazon–Cerrado transition forest by Landsat 5 TM. *Journal of Applied Remote Sensing*, 11(04):1.

[Monteith and Unsworth, 1990] Monteith, J. L. J. L. and Unsworth, M. H. (1990). *Principles of environmental physics*. E. Arnold.

[Papale et al., 2006] Papale, D., Reichstein, M., Aubinet, M., Canfora, E., Bernhofer, C., Kutsch, W., Longdoz, B., Rambal, S., Valentini, R., Vesala, T., and Yakir, D. (2006). Towards a standardized processing of Net Ecosystem Exchange measured with eddy covariance technique: Algorithms and uncertainty estimation. *Biogeosciences*, 3(4):571–583.

[Reichstein et al., 2005] Reichstein, M., Falge, E., Baldocchi, D., Papale, D., Aubinet, M., Berbigier, P., Bernhofer, C., Buchmann, N., Gilmanov, T., Granier, A., Grünwald, T., Havránková, K., Ilvesniemi, H., Janous, D., Knohl, A., Laurila, T., Lohila, A., Loustau, D., Matteucci, G., Meyers, T., Miglietta, F., Ourcival, J.-M., Pumpanen, J., Rambal, S., Rotenberg, E., Sanz, M., Tenhunen, J., Seufert, G., Vaccari, F., Vesala, T., Yakir, D., and Valentini, R. (2005). On the separation of net ecosystem exchange into assimilation and ecosystem respiration: review and improved algorithm. *Global Change Biology*, 11(9):1424–1439.

[Von Randow, 2006] Von Randow, R. C. S.; Alvala, R. C. S. (2006). Estimation of long-wave atmospheric radiation over pantanal sul mato-grossense during the dry seasons of 1999 and 2000. *Brazilian Journal of Meteorology*, pages 398–412.

[Wutzler et al., 2018] Wutzler, T., Lucas-Moffat, A., Migliavacca, M., Knauer, J., Sickel, K., Šigut, L., Menzer, O., and Reichstein, M. (2018). Basic and extensible post-processing of eddy covariance flux data with REddyProc. *Biogeosciences*, 15(16):5015–5030.